Biophysical Journal, Volume *119*

Supplemental Information

The Effect of (−)-Epigallocatechin-3-Gallate on the Amyloid-β Secondary Structure

Atanu Acharya, Julia Stockmann, Léon Beyer, Till Rudack, Andreas Nabers, James C. Gumbart, Klaus Gerwert, and Victor S. Batista

Supplementary Material for The Effect of (−)-epigallocatechin-3-gallate (EGCG) on the Aβ Secondary Structure

Atanu Acharya[1,2], Julia Stockmann[3,4], Léon Beyer[3,4], Till Rudack[3,4], Andreas Nabers[3,4*], James C. Gumbart[1,2], Klaus Gerwert[3,4*], and Victor S. Batista[5*]

[1]School of Physics, Georgia Institute of Technology, Atlanta, Georgia, USA
[2]School of Chemistry and Biochemistry, Georgia Institute of Technology, Atlanta, Georgia, USA
[3] Biospectroscopy, Center for Protein Diagnostics (ProDi), Ruhr University Bochum, Gesundheitscampus 4, 44801 Bochum, Germany
[4]Department of Biophysics, Ruhr University Bochum, Universitätsstrasse 150, 44801 Bochum, Germany
[5]Department of Chemistry, Yale University, New Haven, Connecticut, USA
[*]Correspondence: andreas.nabers@bph.rub.de, gerwert@bph.rub.de, victor.batista@yale.edu

SENSOR FUNCTIONALIZATION

If not mentioned otherwise, chemicals and solutions were purchased from Sigma Aldrich (Germany). All antibodies were obtained from NanoTools (Germany).

In earlier publications the functionalization of the activated sensor surface was already described in detail(1–4). In summary, the internal reflection element (IRE, Germanium) was polished with 0.1 µm grained diamond grinding suspension for 5 min on both sides (Struers A/S, Ballerup, Denmark). After that the crystal was incubated for 10 min in a mixture of hydrogen peroxide and oxalic acid with a relation of 9:1, followed by rinsing with water and drying with nitrogen gas. In these experiments a flow-through cell with a total volume of 600 µl was used, including all connection-tubes. In a first step the sensor surface was incubated with 300 µM N-hydroxysuccinimide-silane dissolved in 2-propanol for 60 min. Unbound silane was removed by rinsing with 2-propanol (5 min), water (2 min) and PBS-buffer (5 min). Afterwards 100 ng/ml monoclonal antibody MOAB-2 solution was flushed over the activated silane surface until saturation was reached, which could be monitored via binding kinetics of the amide II band. Unspecifically attached antibodies were rinsed out by PBS-buffer until an equilibrium of amide II absorbance of remaining antibodies was reached. For blocking of free reactive sites on the surface 0.1 % w/v casein (Sigma, Germany) dissolved in PBS-buffer was used prior to rinsing with PBS-buffer and application of the samples.

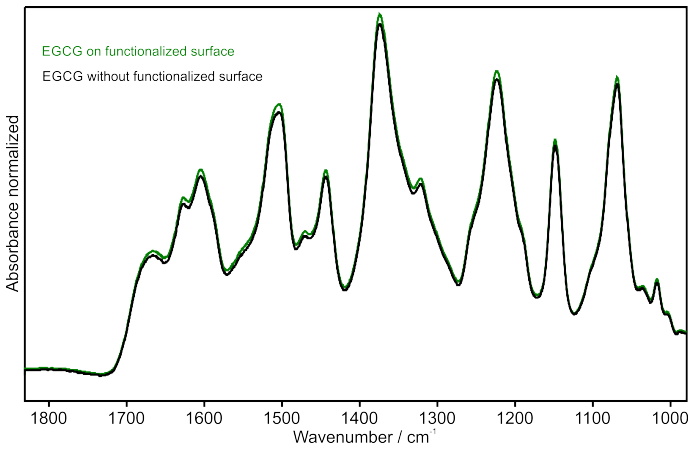

Figure S1: Normalized absorption spectra of EGCG on a functionalized surface (green) and without functionalized surface (black) are almost identical. Therefore, correcting our spectra by subtraction of pure EGCG in solution is valid. Low effect of oxidation in presence of red-light is similar in pure EGCG and EGCG with Aβ; hence they cancel out.

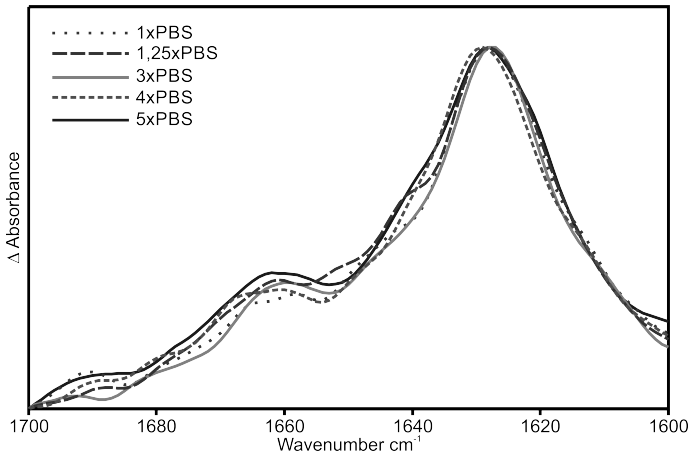

Figure S2: Effect of counter-ion on the secondary structures of Aβ fibrils measured by immuno-infrared-spectroscopy. The results indicate that counter-ions do not affect the $\beta-$sheet enriched fibril secondary structure at all.

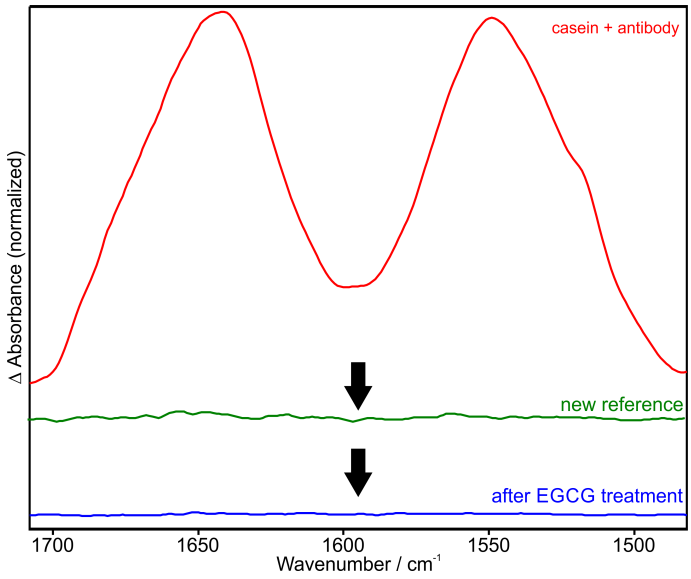

Figure S3: The effect of EGCG on the functionalized immuno-infrared-sensor surface in the absence of Aβ. After sensor functionalization with monoclonal antibody MOAB-2 and subsequent surface saturation (red spectrum) a new reference spectrum was taken. Thus, recording a sample spectrum without any procedural change a baseline spectrum (green spectrum) was recorded. After treatment of the functionalized sensor surface with EGCG followed by subsequent buffer rinsing, we also received a baseline spectrum (blue spectrum) indicating that EGCG did not alter the sensor surface itself. Thus, changes in the amide-I band of Aβ after EGCG treatment are caused by the effect of EGCG on the Aβ secondary structure.

RMSD CALCULATION

Figure S4 shows the RMSD of backbone atoms computed along the 1-μs simulation. We noticed that the RMSD is higher when the top Aβ chain is included in the RMSD calculation. However, RMSD of four chains (except the top one) is much lower. Similar high RMSD values were previously observed for five hIAPP chains in the presence of EGCG (5).

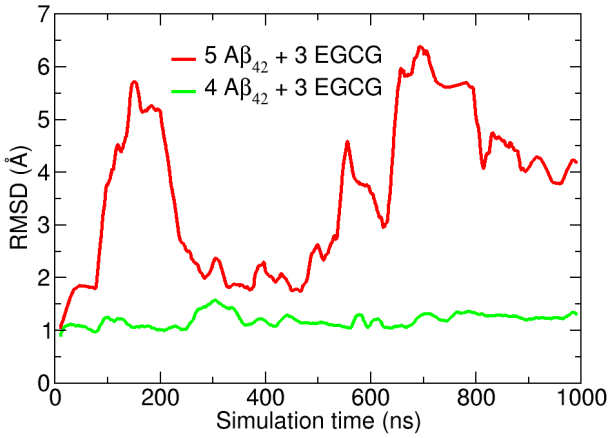

Figure S4: RMSD of Aβ backbone atoms along 1-μs MD simulation.

DOCKING CALCULATIONS

We optimized the EGCG molecule at B3LYP/6-31+g(d,p) level of theory in implicit water model. The optimized EGCG was used for docking calculation on an Aβ fibril. Docking calculations were performed using the Schrödinger suite (6). We applied the GLIDE (7) protocol (GlideScore version SP5.0) to find docking sites using single precision (SP), including an exhaustive search for docking sites around and inside the Aβ structure. We performed four independent calculations centered around four parts of the Aβ structures to include the entire structure of the Aβ in docking. In each case, we request five best poses of EGCG. Only three of these four docking calculations resulted in docking poses: one at each terminal and one inside (site #1). Among five poses from each of these three docking sites, we picked the best pose (for each site) by the most negative glide score. Subsequent MD simulation was initiated using the best pose for three EGCG molecules from three docking sites.

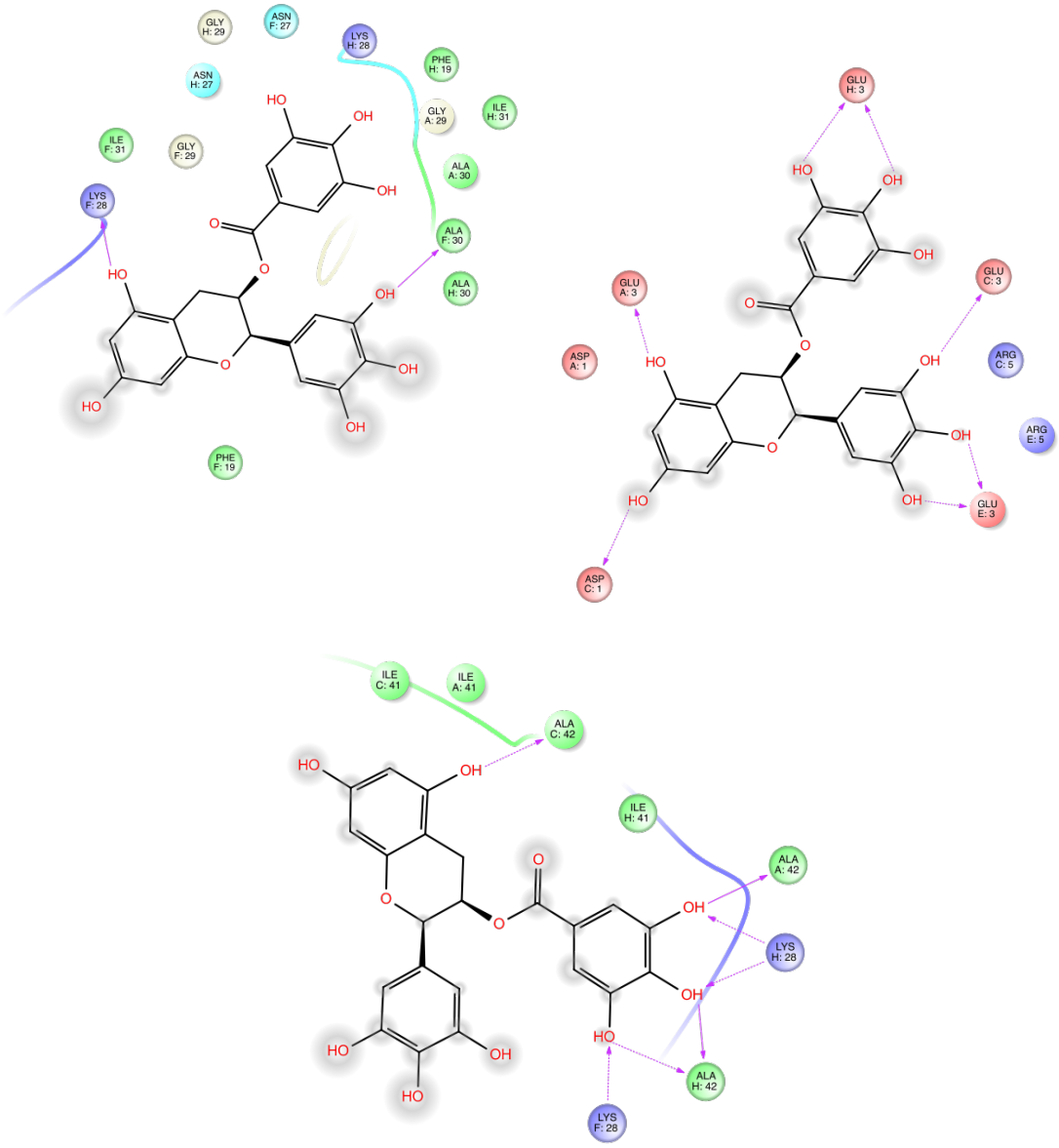

Figure S5: EGCG interactions with Aβ_{42} residues for docking site #1 (top left), #2 (top right), and #3 (bottom) as obtained from Maestro.

REFERENCES

1. Nabers, A., L. Perna, J. Lange, U. Mons, J. Schartner, J. Güldenhaupt, K. U. Saum, S. Janelidze, B. Holleczek, D. Rujescu, O. Hansson, K. Gerwert, and H. Brenner, 2018. Amyloid blood biomarker detects Alzheimer's disease. *EMBO Mol. Med.* 10:e8763.

2. Schartner, J., A. Nabers, B. Budde, J. Lange, N. Hoeck, J. Wiltfang, C. Kötting, and K. Gerwert, 2017. An ATR-FTIR-Sensor Unraveling the Drug Intervention of Methylene Blue, Congo Red, and Berberine on Human Tau and Aβ. *ACS Med. Chem. Lett.* 8:710–714.

3. Nabers, A., J. Ollesch, J. Schartner, C. Kötting, J. Genius, H. Hafermann, H. Klafki, K. Gerwert, and J. Wiltfang, 2016. Amyloid-β-secondary structure distribution in cerebrospinal fluid and blood measured by an immuno-infrared-sensor: A biomarker candidate for Alzheimer's disease. *Anal. Chem.* 88:2755–2762.

4. Nabers, A., J. Ollesch, J. Schartner, C. Kötting, J. Genius, U. Haußmann, H. Klafki, J. Wiltfang, and K. Gerwert, 2016. An infrared sensor analysing label-free the secondary structure of the Abeta peptide in presence of complex fluids. *J. Biophotonics* 9:224–234.

5. Wang, Q., J. Guo, P. Jiao, H. Liu, and X. Yao, 2014. Exploring the influence of EGCG on the β-sheet-rich oligomers of human islet amyloid polypeptide (hIAPP1–37) and identifying its possible binding sites from molecular dynamics simulation. *PLoS One* 9:1–12.

6. Schrödinger, LLC, New York, 2017. Small-Molecule Drug Discovery Suite.

7. Friesner, R. A., R. B. Murphy, M. P. Repasky, L. L. Frye, J. R. Greenwood, T. A. Halgren, P. C. Sanschagrin, and D. T. Mainz, 2006. Extra precision glide: Docking and scoring incorporating a model of hydrophobic enclosure for protein- ligand complexes. *J. Med. Chem.* 49:6177–6196.